Three-dimensional horizontal circular spiral photonic crystals with stop gaps below 1 μm

Kock Khuen Seet, Vygantas Mizeikis, Saulius Juodkazis, and Hiroaki Misawa[a)]
Core Research for Evolution Science and Technology (CREST), Japan Science and Technology Corporation (JST) and Research Institute for Electronic Science, Hokkaido University, North 21, West 10, CRIS Building, Kita-ku, Sapporo 001-0021, Japan

(Received 1 November 2005; accepted 15 April 2006; published online 30 May 2006)

Three-dimensional photonic crystals with a circular spiral architecture were fabricated by direct laser writing (DLW) in a photoresist. DLW was performed with a laser beam having the direction of propagation and elongation of the ellipsoidal focal region perpendicular to the spirals' orientation. This allowed the reduction of the turning period of the spirals while avoiding the overlap between their adjacent turns. Consequently, optical transmission and reflection spectra of the fabricated samples revealed multiple photonic stop gaps whose shortest wavelength was 0.88 μm, the lowest observed so far in spiral structures. These results were qualitatively reproduced by finite-difference time-domain simulations. This fabrication scheme can be useful for DLW of structures where photonic stop gaps along particular directions, rather than complete photonic band gaps, are required. © *2006 American Institute of Physics*. [DOI: 10.1063/1.2207841]

Photonic crystals are periodic microstructures with a spatial modulation in their refractive index in specific directions. This modulation leads to the opening of photonic band gaps (PBG) or stop gaps where the propagation of electromagnetic waves is forbidden within certain frequency ranges.[1,2] In recent years the fabrication of photonic crystals using direct drawing by focused femtosecond laser beams in liquid resins and photoresists via two-photon absorption (TPA) has received much attention.[3–7] The main merit of this direct laser writing (DLW) technique stems from its ability to produce almost any kind of three-dimensional architecture. With the selection of an appropriate photosensitive material having a threshold response, recording at subdiffraction limit resolution can be achieved.[8] Thus, DLW is ideal for three-dimensional photonic crystals with intricate periodic architectures, such as the diamond lattice,[9,10] slanted pores,[11,12] and spiral diamond[13,14] structures, which are difficult or impossible to realize by other known techniques. Among these proposed architectures for photonic crystals, the spiral structure is an attractive candidate that has been proposed on the basis of its large PBG derived from its strong diamond connectivity.[15] Recently these periodic spiral structures have been fabricated by two-photon laser writing in a negative-tone photoresist. Optical characterization indicates that stop gaps exist in the midinfrared region (between 2 and 6 μm).[14] Scaling the band gaps toward shorter wavelengths in the telecommunication and visible regions is a highly desirable and constantly sought goal for many proposed fabrication schemes. For spiral structures, such scaling can be implemented by reducing the lattice period (a) or the spiral pitch (c) [see Fig. 1(a)]. Unfortunately, when the spirals are drawn by the laser beam focused along the Z axis as shown in the inset of Fig. 1(b), the elongated shape of the photopolymerized volume element (voxel), derived from the ellipsoidal shape of the focal region, makes downscaling of the spiral pitch difficult without excessive overlapping of the spiral arms. This problem is also encountered in the so-called woodpile architecture, where the ellipsoidal photopolymerized volume inhibits further scaling down of the interdistance between adjacent stacked logpiles,[6,7] which is required for the face-centered-cubic (fcc) unit cell. For a photoresist such as SU-8, which works by step-growth polymerization and is designed for high-resolution recording,[16] an additional problem is image blurring which occurs when photoacid diffusion[17] causes nearby features to merge and makes further downscaling of the lattice period extremely difficult. Nanorods with lateral dimensions of 30 nm,[18] obtained by carefully controlling the exposure dose to marginally above the photomodification threshold, provide answers to the resolution limit of two-photon writing in SU-8 but remain difficult to implement for actual fabrication. Since acid diffusion is intrinsic to a chemically amplified resist and is estimated to be on the order of several tenths of a nanometer,[17] the current resolution obtained for isolated spots (120 nm) (Ref. 8) and extended structures (180 nm) (Ref. 6) may already represent the near optimum of subdiffraction limit for practical implementation. Hence the realization of structures with spatial index modulations across distances smaller than a few hundred nanometers will have to rely on the development of new laser sources and resists.

As an alternate approach, we report here a fabrication scheme to construct spiral structures such that the spiral advancing direction (spiral axis) is horizontal or perpendicular

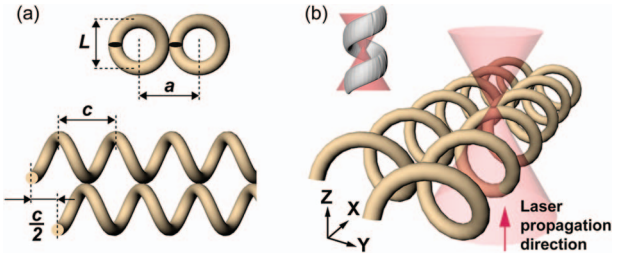

FIG. 1. (Color) (a) Definition of basic spiral parameters. (b) Fabrication of horizontal spirals. The inset shows the fabrication of vertical spiral.

[a)]Author to whom correspondence should be addressed; electronic mail: misawa@es.hokudai.ac.jp

to the beam focusing direction [see Fig. 1(b)]. Since the lateral size of the voxel is about one-third its axial size, a smaller pitch c can be chosen. Although this modification does not affect the voxel volume, its different orientation helps to avoid excessive overlap within the spirals. Using this approach, various structures were fabricated with the spiral pitch varying from 0.8 to 1.12 μm, and their optical characterization revealed stop gaps with sizeable attenuation of about 15%–60% in the spectral interval of 0.88–3.1 μm.

Figure 1(b) illustrates schematically the DLW of horizontal spirals. The laser beam is focused along the axis orthogonal to the spiral advancing direction. The adjacent circular spirals are phase shifted by half a spiral pitch period ($c/2$) in accordance with the proposed model.[19] This phase shift is also necessary to create more contact points between the adjoining spiral columns to minimize lattice distortion during the chemical development and drying processes where strong structural loading is encountered. The fabrication setup consists of the laser source, an optical microscope housing the objective lens [numerical aperture (NA)=1.35, 100×], and a three-dimensional (3D) piezoelectric transducer scanning stage assembly. The output of the laser system (central wavelength $\lambda=800$ nm, pulse width $\tau_{\text{pulse}}=150$ fs, and repetition rate $f=100$ Hz) is attenuated by variable attenuators for adjusting the pulse energy to trigger irreversible photochemical reactions within the sample photoresist (typically <1 nJ). The sample used is SU-8 (Microchem) spin coated on glass substrate to a typical thickness of 25 μm. The stage is translated according to predefined data points to inscribe the spiral patterns during the recording phase. The objective lens tightly focuses the femtosecond laser pulses to a very confined volume within the sample, and the irradiated focal region reaches a high photon density, which facilitates two-photon absorption by the photoinitiators to generate the photoacids. Since the TPA rate is proportional to the square of the local light intensity, its spatial distribution is much sharper than that of light intensity at the focal spot.[8,18] In SU-8, the gelation process is abrupt with respect to the density of polymer that is cross-linked due to TPA. All these circumstances make possible DLW with subdiffraction limit resolution. As SU-8 is a negative-tone epoxy-based photoresist that works by cationic photopolymerization, the cross-linking is initiated thermally during the postbake process at the sites where the photoacids are produced. A subsequent chemical development transforms the recorded latent image into the dielectric periodic structure by removing the non-cross-linked regions of the initial material.

Using the procedures described above, periodic structures of horizontal circular spirals with adjacent spiral columns phase shifted by $c/2$ were fabricated in SU-8, whose scanning electron microscopy (SEM) micrographs are shown in Fig. 2. The structure shown has a lateral size of 40 μm (width)×31 μm (depth) and a height of 20 μm, with 28 spiral periods (n_x) in a single spiral column [Fig. 2(a)], and takes about 1.5 h to construct. Various structures were constructed with the same width and height but with varying spiral pitches c of 0.8, 0.9, 1.0, and 1.12 μm, hence the depth changes while the number of spiral periods n_x is kept unchanged. The front view (looking toward the X axis) of the spiral [Fig. 2(d)] differs from the ideal circular profile; it has a hollow center, as illustrated in Fig. 1(a), due to the ellipsoidal-shaped focal volume, and results in a higher filling ratio. To avoid excessive overlapping and a too high

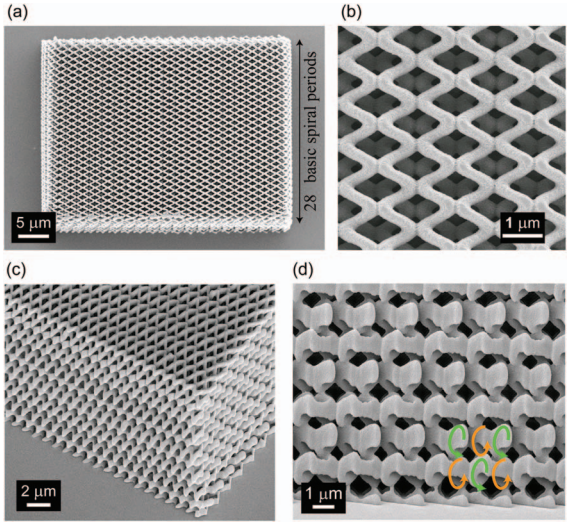

FIG. 2. (Color) SEM micrographs. (a) Overall top view. (b) Enlarged top view with visible phase-shifted adjacent layer underneath. (c) Perspective view revealing the spirals propagating in the horizontal direction parallel to the substrate. (d) Closed-up frontal view (green and orange arrows indicating adjacent spiral columns). Same-colored labels indicate identical phase.

filling ratio, the spacing between the spirals stacked in the Z direction is increased to 1.4 μm to account for the elongation in the focusing direction, while the lateral spacing between adjacent spirals in the Y direction is kept at 1 μm. Using these parameters, the adjoining spiral columns are arranged such that they are barely in contact with each other [Fig. 2(b)]. The extended structures are structurally stable and self-supporting, as evident from Fig. 2(c).

The structures were optically characterized by transmission and reflection spectral measurements using a Fourier-transform infrared (FT-IR) spectrometer with a microscopic attachment (6000TM-M with IRT-3000, JASCO). Spectral measurements were taken along the X direction, which is along the spiral axis direction, by mounting the sample on a custom-made holder and stage assembly that has five degrees of freedom consisting of three translations and two rotations (about the X and Y axes). Lateral imaging of the side surface [indicated by the arrow in the inset of Fig. 3(a)] is used as a guide for alignment of the spiral structures for the FT-IR measurements. For various values of c, reflectance peaks of 15%–20% were observed that scaled from 1.2 to 0.88 μm as the spiral pitch was reduced [Fig. 3(a)]. This is in accordance with Maxwell's scaling law, and indicates that photonic stop gaps are present in the fabricated structures. To the best of our knowledge, these stop gaps have the shortest wavelengths (below 1 μm) observed so far in spiral structures. Simultaneously, they exhibit reasonable attenuation of 15%. It is likely that at these wavelength measurements by the micro-FT-IR technique yield transmission and reflection features weaker than the actual ones due to the notable spread of the incidence angles in the Cassegrainian objective. Also, previous works on higher-order gaps at around 1 μm have diminished magnitudes.[12,20] Horizontal spiral structures with 0.6 μm pitch were also fabricated successfully, and a very weak stop gap (~3%) at 0.78 μm, which is inside the visible region, was observed. However, at such a small pitch the spiral turns begin to overlap each other, and the large signal-to-noise ratio begins to interfere with the appearance of the stop gap at such short wavelengths (limits of instrumenta-

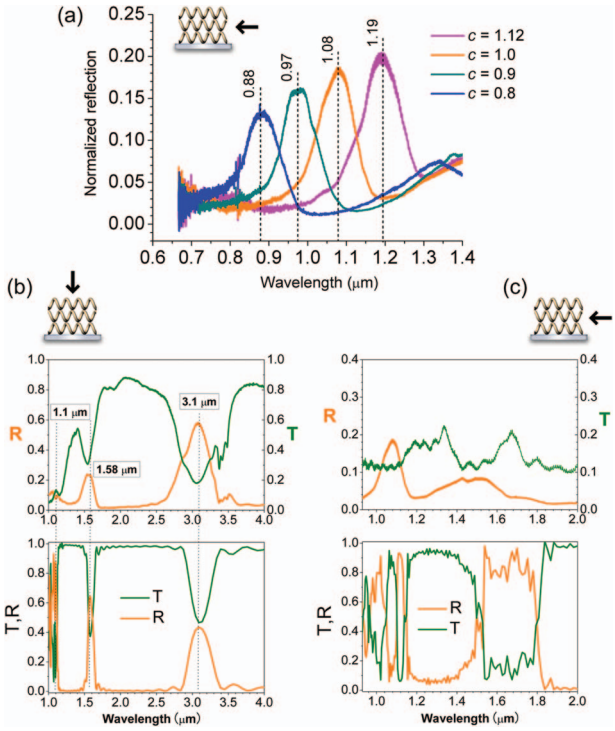

FIG. 3. (Color) (a) FT-IR measured results for structures with various spiral pitches. [(b) and (c)] Comparison of measured and theoretical spectral results taken in the direction as indicated by the inset.

tion). Figures 3(b) and 3(c) show the spectra measured along the *X*-axis and *Z*-axis directions [parallel and perpendicular to the spiral axes, respectively (see inset)], and a comparison with theoretical spectra calculated by the finite-difference time-domain (FDTD) technique. The FDTD calculation directly solves Maxwell's equations on a 3D rectangular grid, with the finite differences replacing the partial derivatives. The dielectric environment for the calculation was defined by direct simulation of the DLW process: strongly overlapping dielectric ellipsoids with a refractive index of $n=1.6$ were generated along the spiral trajectories. As a result, smooth dielectric spirals were generated. A plane-wave broadband pulse was used to probe the structure's optical response. Orientations and geometric parameters of the ellipsoids and spirals as well as the probing beam direction were chosen to match the actual situation. In the plane perpendicular to the probing direction, the FDTD domain spanned one unit cell with periodic boundary conditions, while along the probing direction it spanned the required number of spiral periods with perfectly matched layer boundary conditions. Good qualitative agreement was seen between the experiment and simulations in the *Z*-axis direction [Fig. 3(b)]. The matching for the fundamental peak at 3.0 μm is almost quantitative. The trailing down toward shorter wavelengths in the measured spectra is attributed to scattering effects. Along the *X* axis, the peak at the shorter wavelength near 1.1 μm is also observed in both measured and calculated results, but the measured peak is blueshifted slightly by about 0.1 μm. The difference likely comes from experimental factors, such as some nonuniformities in the spirals, and from the spread of the incidence angles in the optical characterization. Nevertheless, the qualitative agreement is still present in this case.

In conclusion, we have implemented a scheme to fabricate photonic crystals based on the spiral architecture by using the DLW technique, which enables a larger adjustment range and downscaling for the spiral pitch. This method allowed us to fabricate photonic crystal templates with stop gaps within 0.88–3.1 μm wavelength range with a reasonable degree of optical attenuation. This fabrication scheme can be considered for use in the design of structures for applications where photonic stop gaps along particular directions, rather than complete PBGs, are necessary. It may also prove useful for building architectures with other point lattice types, such as the [001]-fcc structures.[21]

[1]E. Yablonovitch, Phys. Rev. Lett. **58**, 2059 (1987).
[2]S. John, Phys. Rev. Lett. **58**, 2486 (1987).
[3]H.-B. Sun, S. Matsuo, and H. Misawa, Appl. Phys. Lett. **74**, 786 (1999).
[4]H.-B. Sun, V. Mizeikis, Y. Xu, S. Juodkazis, J.-Y. Ye, S. Matsuo, and H. Misawa, Appl. Phys. Lett. **79**, 1 (2001).
[5]J. Serbin, A. Egbert, A. Ostendorf, B. N. Chichkov, R. Houbertz, G. Domann, J. Schulz, C. Cronauer, L. Fröhlich, and M. Popall, Opt. Lett. **28**, 301 (2003).
[6]M. Deubel, G. V. Freymann, M. Wegener, S. Pereira, K. Busch, and C. M. Soukoulis, Nat. Mater. **3**, 444 (2004).
[7]V. Mizeikis, K. K. Seet, S. Juodkazis, and H. Misawa, Opt. Lett. **29**, 2061 (2004).
[8]T. Tanaka, H.-B. Sun, and S. Kawata, Appl. Phys. Lett. **80**, 312 (2002).
[9]R. Bitwas, C. T. Chan, M. Sigalas, C. M. Soukoulis, and K. M. Ho, in *Photonic Band Gap Materials*, edited by C. M. Soukoulis (Kluwer, Dordrecht, 1995).
[10]K. Kaneko, H.-B. Sun, X.-M. Duan, and S. Kawata, Appl. Phys. Lett. **83**, 2091 (2003).
[11]O. Toader, M. Berciu, and S. John, Phys. Rev. Lett. **90**, 233901 (2003).
[12]M. Deubel, M. Wegener, A. Kaso, and S. John, Appl. Phys. Lett. **85**, 1895 (2004).
[13]O. Toader and S. John, Science **292**, 1133 (2001).
[14]K. K. Seet, V. Mizeikis, S. Matsuo, S. Juodkazis, and H. Misawa, Adv. Mater. (Weinheim, Ger.) **17**, 541 (2005).
[15]M. Maldovan and E. L. Thomas, Nat. Mater. **3**, 593 (2004).
[16]C. H. Lee, T. W. Chang, K. L. Lee, J. Y. Lin, and J. Wang, Appl. Phys. A: Mater. Sci. Process. **79**, 2027 (2004).
[17]R. C. Rumpf and E. G. Johnson, J. Opt. Soc. Am. A **21**, 1703 (2004).
[18]S. Juodkazis, V. Mizeikis, K. K. Seet, M. Miwa, and H. Misawa, Nanotechnology **16**, 1 (2005).
[19]A. Chutinan and S. Noda, Phys. Rev. B **57**, R2006 (1998).
[20]M. Straub, M. J. Ventura, and M. Gu, Phys. Rev. Lett. **91**, 043901 (2003).
[21]O. Toader and S. John, Phys. Rev. E **66**, 016610 (2002).